



**Thiol-promoted catalytic synthesis of high-performance
furan-containing lubricant base oils from biomass derived
2-alkylfurans and ketones**

Journal:	<i>Green Chemistry</i>
Manuscript ID	GC-ART-06-2020-001897.R1
Article Type:	Paper
Date Submitted by the Author:	16-Sep-2020
Complete List of Authors:	Liu, Sibao; Catalysis Center for Energy Innovation, Department of Chemical and Biomolecular Engineering; The University of Delaware Bhattacharjee, Rameswar; University of Delaware, Chemical and Biomolecular Engineering Li, Sha; University of Delaware Danielson, Andrew; University of Delaware Mazal, Tobias; University of Delaware Saha, Basudeb; University of Delaware, Catalysis Center for Energy Innovation; Vlachos, Dion; Univ. of Delaware,

Thiol-promoted catalytic synthesis of high-performance furan-containing lubricant base oils from biomass derived 2-alkylfurans and ketones

Sibao Liu^{1,2}, Rameswar Bhattacharjee¹, Sha Li¹, Andrew Danielson^{1,3}, Tobias Mazal^{1,3}, Basudeb Saha^{1*}, and Dionisios G. Vlachos^{1,3*}

¹Catalysis Center for Energy Innovation, University of Delaware, 221 Academy St., Newark, DE 19716, USA

²Current address: Key Laboratory for Green Chemical Technology of Ministry of Education, School of Chemical Engineering and Technology, Tianjin University, Tianjin 300072, China

³Department of Chemical and Biomolecular Engineering, University of Delaware, 150 Academy St., Newark, DE 19716, USA

Abstract

About 97% of lubricant base oils are currently sourced from petroleum and the majority of the rest is produced from vegetable oils. We demonstrate a promising catalytic route to produce base oils from lignocellulosic biomass-derived 2-alkylfurans and ketones via carbon-carbon coupling in neat condition. Among several homogeneous and heterogeneous acid catalysts tested, a perfluorinated sulfonic acid (Aquivion PW79S) exhibits the best catalytic performance and yields up to 90% renewable furan-containing base oils with the use of a thiol promotor. The effects of the acid strength of the catalysts, molecular size and structure of thiols and ketones, and fraction of thiols are studied. Electronic structure calculations elucidate the reaction pathway and indicate that the thiol reduces the barrier of the rate-determining dehydration step. The structure and properties of base oils can be tuned by using different synthons. These base oils have excellent properties and can be competitive with or surpass the commercial synthetic alkylnaphthalene and furan-containing bio-ester base oils.

*Corresponding authors: vlachos@udel.edu, bsaha@udel.edu

1. Introduction

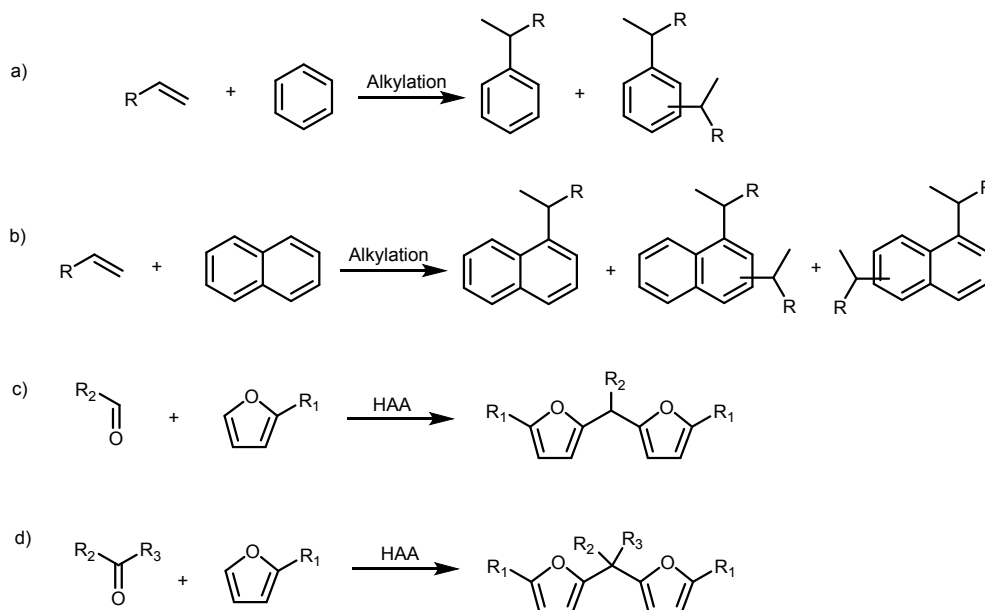
Lubricant production from alternative feedstock, *e.g.* biomass, has received considerable interest to mitigate global environmental challenges. Lubricants are widely used in industry, automobiles, aviation machinery, refrigeration compressors, and several other applications¹⁻⁵. Base oils are the key component of lubricants (up to 90% by weight) and significantly influence their properties⁶. Currently, natural oils-derived bio-ester base oils are only produced from non-conventional feedstock. The bio-ester lubricants have limited applications because of their low oxidative stability at high temperatures, low hydrolytic stability and poor pour point (PP)⁶. In contrast, hydrocarbon base oils, such as mineral oils, synthetic poly- α -olefins (PAOs), and alkylated aromatic base oils do not possess such problems⁶. The synthetic PAOs and alkylated aromatic base oils also possess better properties than mineral oils. Alkylated aromatic base oils, *e.g.*, alkylbenzene and alkylnaphthalene, have additional advantages, such as higher polarity stemming from their electron-rich aromatic rings, which enable improved solubility and dispersion with polar additives, sludge, and degradation products that are either added during lubricant formulation or formed during use⁶. The industrial processes to manufacture aromatic base oils (*e.g.*, alkylbenzene base oils by Sasol, Hunstamn Corp., and Petresa Canada and alkylnaphthalene base oils by ExxonMobil Chemical Company and King Industries, Inc.) employ highly corrosive acid catalyzed (HF, AlCl₃, trifluoromethane sulfonic acid) Friedel-Crafts reaction with petroleum-derived benzene, naphthalene and olefins (Schemes 1a and 1b)⁶. Control of product selectivity with these homogeneous acid catalysts is challenging. Thus, development of novel catalytic processes to produce biomass-derived base oils with tunable properties is desirable to for high performance lubricants for modular and energy-efficient machinery and equipment.

Ketones can be widely sourced from biomass *via* chemical or biological catalysis or hybrid routes (Scheme S1). For example, acetone, 2-nonanone, 2-undecanone, and 2-tridecanone can be produced *via* microbial fermentation⁷⁻¹¹. Ketones, of different chain length, also can be produced by catalytic alkylation of methyl ketones with biomass derived alcohols^{12, 13}. Ketonization of carboxylic acids, obtained from biomass and natural oils, can also provide ketones in high yield¹⁴⁻¹⁶. Dehydrogenation of biomass derived mono-secondary alcohols, such as 2-butanol¹⁷, 2- or 3-pentanol¹⁸ and 2- or 3-hexanol¹⁹, can produce their corresponding ketones including 2-butanone, 2- or 3-pentanone and 2- or 3-hexanone. Hydrogenolysis of biomass derived 2,5-dimethylfuran and 2-methylfuran can produce 2-hexanone and 2-pentanone, respectively, with high selectivity^{20, 21}. Cyclic ketones, such as 4-propyl cyclohexanone, can be produced from lignin phenols by hydrogenation and dehydrogenation^{22, 23}. Production of biomass substrates, such as 5-hydroxymethylfurfural (HMF), furfural, furan, 2-alkylfurans, 2,5-furandicarboxylic acid (FDCA)²⁴ has been reported extensively (Scheme S2). For example, HMF and furfural can be produced from lignocellulosic biomass by hydrolysis and dehydration^{25, 26}. FDCA is obtained from catalytic oxidation of HMF²⁷. Methylfuran can be derived from direct hydrodeoxygenation (HDO) of furfural, a dehydration product of hemicellulosic xylose^{28, 29}. Long chain 2-alkylfurans can be produced *via* acylation of furan with carboxylic acids or anhydrides and subsequent HDO of the acylated intermediates³⁰.

C-C coupling of bio-based ketones and furanic compounds to produce high carbon number hydrocarbons and aromatic base oils has been reported recently. For example, Bell and co-

workers reported the synthesis of aromatic and cycloalkane base oils from bio-based ketones via self-condensation and hydrogenation/HDO of condensation intermediates³¹⁻³³. Although some of the properties of these base oils are comparable to those of synthetic PAOs, their viscosities are relatively higher than those PAOs, and this is undesirable from an energy efficiency standpoint. In addition, a high temperature (190 °C) was employed for the self-condensation. Wang et al. introduced a four-step method, combining aldol condensation of furfural with acetone, hydrogenation, aldol condensation of hydrogenated ketone intermediates with furfural and finally HDO, to produce base oils. The yield of the C₂₃ branched alkane was only 50% and its properties were not reported³⁴. In addition, the aldol condensation step poses separation and disposal challenges of the homogeneous catalysts. Fan et al. synthesized a furan ring containing bio-ester base oil, isooctyl furan dicarboxylate, *via* esterification of FDCA and 2-ethylhexanol over *p*-toluenesulfonic acid (*p*-TSA)³⁵. This furan-containing ester base oil shows comparable thermal and oxidative stability to the synthetic ester base oils, isooctyl sebacate, and better friction-reducing and anti-wear properties. However, the viscosity index (VI) and PP are inferior to isooctyl sebacate.

We have recently reported the synthesis of a new type of furan-containing lubricant base oil *via* hydroxylalkylation/alkylation (HAA) of bio-based 2-alkylfurans and aldehydes (Scheme 1c)³⁶. This lubricant base oil has better VI and PP than the commercial alkylnaphthalene base oil, make it promising for low temperature applications³⁶. In this paper, we study HAA of 2-alkylfurans with ketones to produce furan-containing base oils for the first time (Scheme 1d). Mechanistically, HAA of 2-alkylfurans with ketones is harder than that with aldehydes because the carbonyl group of ketones is less electrophilic and steric crowding is greater. The HAA coupling of 2-alkylfurans and various ketones is carried out over a series of sulfonic acid catalysts promoted by various thiols. The properties of the synthesized base oils, such as the kinematic viscosity at 40 and 100 °C (KV40, KV100), VI, PP, oxidation stability and volatility, are measured and compared with those of commercial petroleum-derived alkylnaphthalene base oils and other furan-containing base oils.



Scheme 1. Approaches to synthesize various alkylated aromatics and furan base oils: industrial route for the production of alkylbenzene (a) and alkylnaphthalene (b) base oils and our approach to renewable furan-containing base oils by hydroxyalkylation/alkylation (HAA) of 2-alkylfurans with aldehydes (c) or ketones (d).

2. Experimental

2.1 Chemicals and materials

Aquivion® PW79S (coarse powder), Aquivion® PW98 (coarse powder), Amberlyst®-15 (dry hydrogen form), methanesulfonic acid ($\geq 99.0\%$), *p*-toluenesulfonic acid monohydrate ($\geq 98.5\%$), and triflic acid ($\geq 99.0\%$) were purchased from Sigma-Aldrich. Amberlyst® 36 dry resin was produced by Rohm and Haas. 5 M H₂SO₄ was purchased from Fluka. 2-Pentylfuran ($\geq 98.0\%$), 2-undecanone (99%), 1-propanethiol (99%) and eicosane (99%) were purchased from Sigma-Aldrich. 4-Undecanone ($>95\%$), 6-undecanone ($>98\%$), 2-hexanone ($>98\%$), 2-nonanone ($>98\%$), 1-butanethiol ($>97\%$), *tert*-butyl mercaptan ($>98\%$), hexyl mercaptan ($>96\%$), 1-octanethiol ($>98\%$), cyclohexanethiol ($>98\%$), benzyl mercaptan ($>96\%$), and diethyl sulfide ($>98\%$) were purchased from Tokyo Chemical Industry Co., Ltd. Cyclohexane (99.9%) was purchased from Fisher Chemical.

2.2 Activity tests and analytical methods

The HAA reaction was carried out in a glass vial equipped with a magnetic stirrer. In a typical reaction, 4 mmol 2-alkylfuran and 2 mmol ketone (neat) and a certain amount of catalyst were used. The vial was placed in a preheated oil bath and stirred at 500 rpm using a magnetic bar on a stirring hotplate. After reaction for a desired time, the aliquot was diluted using 10 ml cyclohexane as a solvent for gas chromatography (GC) analysis. A small amount of eicosane was added to the solution as an internal standard.

The products were analysed by a GC (Agilent 7890A) equipped with an HP-1 column and a flame ionization detector (FID). The products were identified by a GC (Agilent 7890B) mass spectrometer (Agilent 5977A with a triple-axis detector) equipped with a DB-5 column. High resolution mass spectrometry-liquid injection field desorption ionization (HRMS-LIFDI, Waters GCT Premier) data were obtained from the Mass Spectrometry Facility at the University of Delaware. ¹H NMR and ¹³C NMR spectra were recorded on a Bruker AV400 NMR (400 MHz) equipped with a cryogenic Quattro Nucleus Probe (QNP). Chloroform-*d* was used as a solvent for the NMR studies. For the ¹H NMR analysis, the chemical shifts for proton signals are reported in parts per million (ppm) with reference to the solvent peak. ¹³C NMR was fully decoupled by broad-band proton decoupling and the chemical shifts are reported in ppm with reference to the center line of a triplet at 77.16 ppm of chloroform-*d*.

The conversion and the yield of all products from HAA reactions were calculated on carbon basis using the following equations:

$$\text{Conversion [\%]} = \frac{\text{mol of initial reactant} - \text{mol of unreacted reactant}}{\text{mole of initial reactant}} \times 100$$

$$\text{Yield of detected products [\% - C]} = \frac{\text{mol}^{\text{product}} \times \text{C atoms in product}}{\text{mol of total C atoms of initial reactants}} \times 100$$

2.3 Lubricant properties measurements

The lubricant properties of synthesized base oils were determined by ASTM methods at Southwest Research Institute (San Antonio, Texas, USA). The kinematic viscosities at 100 °C and 40 °C (KV100 and KV40) were determined using the ASTM D445 method. The VI was

calculated from KV100 and KV40 using the ASTM D2270 method. The PP was measured with the ASTM D97 method.

2.4 Computational methods

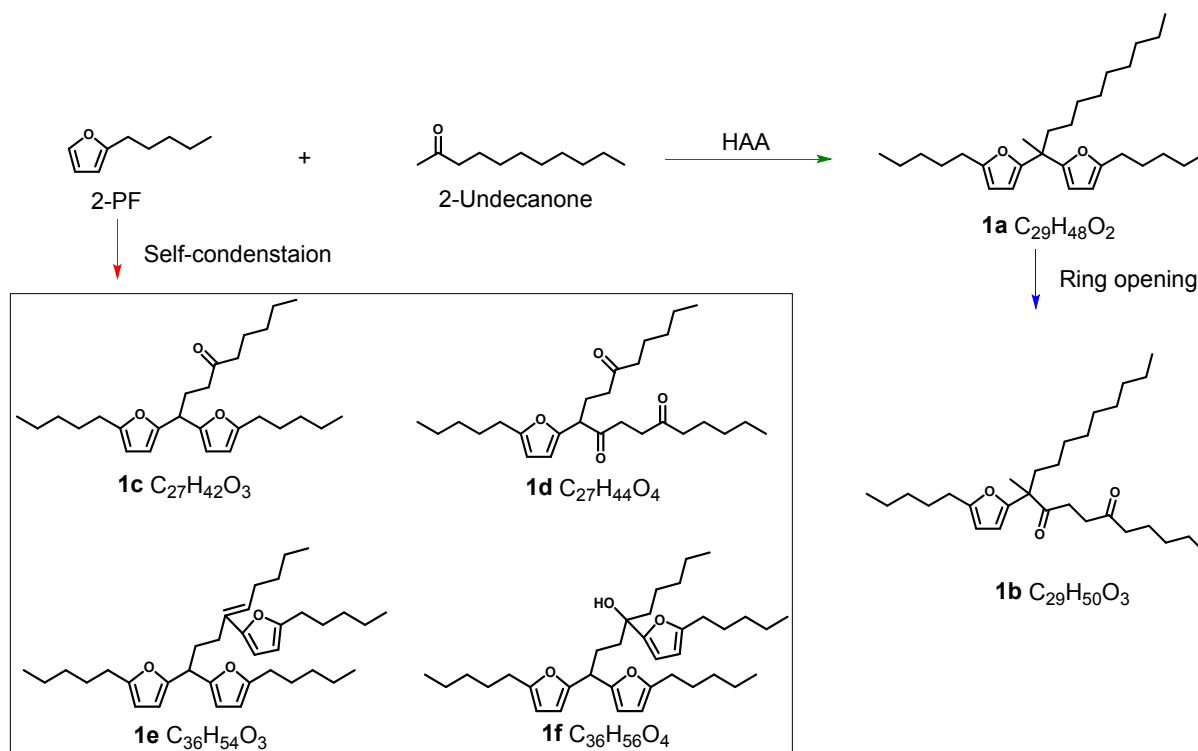
All electronic structure calculations were performed with Gaussian 09³⁷ with default convergence settings for the SCF and Berny optimization cycles at the M062X/6-311G(2df,pd) theory level. Ground and transition states were confirmed by vibrational frequency analysis and intrinsic reaction coordinate (IRC) calculations. Thermal corrections to the electronic energies are computed within the harmonic oscillator approximation.

3. Results and Discussion

3.1 Catalyst screening for HAA reaction

Initially, we target synthesis of a C₂₉ furan base oil (referred hereto as C₂₉-FL) from 2-pentylfuran (2-PF) and 2-undecanone for the following reasons: (1) commercial alkylnaphthalene base oils typically contains 20-50 carbon atoms, and (2) bio-based 2-undecanone and 2-PF can be synthesized *via* alkylation of 1-octanol with acetone³³ and acylation of furan with valeric acid or valeric anhydride followed by HDO³⁰, respectively. First, two perfluorinated sulfonic acid resin catalysts, Aquivion PW98 and Aquivion PW79S, were chosen for the HAA reaction without any thiol because of their excellent catalytic performance in our prior studies of 2-PF with aldehydes³⁶ and enals³⁸. In the absence of a thiol, a large amount of 2-undecanone (conversion <57%) remain unconverted at >92% 2-PF conversion (Table 1, entries 1 and 2), a fact attributed to the less electrophilic carbonyl group of ketones. High 2-PF conversion is likely due to its self-oligomerization. At a 2 to 1 molar ratio of 2-PF and 2-undecanone, the HAA product (C₂₉H₄₈O₂, **1a**) dominates (Scheme 2). Small fractions of other products form *via* ring opening of the HAA product (C₂₉H₅₀O₃, **1b**) and self-condensation of 2-PF (C₂₇H₄₂O₃, **1c**, C₂₇H₄₄O₄, **1d**, C₃₆H₅₄O₃, **1e** and C₃₆H₅₆O₄, **1f**). Aquivion PW79S achieves higher formation rate and higher yield (49%) to product **1a** than Aquivion PW98 because of its higher acid density³⁸.

The above reactions with 1-propanethiol as a promoter at 1:1 molar ratio with H⁺ (catalyst) exhibit significantly increased conversion of 2-undecanone and formation rates and yields of **1a** (Table 1, entries 3 and 4). For example, the reaction catalyzed by Aquivion PW79S and 1-propanethiol results in 78% conversion of 2-undecanone and 72% yield of **1a** (Table 1, entry 3). The formation rate of **1a** is 16.8 mol·mol_{H⁺}⁻¹·h⁻¹, which is about 1.5 times higher than that obtained without 1-propanethiol. 1-propanethiol alone does not catalyze the reaction, which indicates that 1-propanethiol cooperates with the catalysts. Several liquid and solid sulfonic acid catalysts were screened in the presence of 1-propanethiol. The formation rates follow the order of CF₃SO₃H > *p*-TSA > CH₃SO₃H for homogeneous catalysts, and perfluorinated sulfonic acid resins (Aquivion PW79S and Aquivion PW98) > solid sulfonic-acid-functionalized cross-linked polystyrene resins (Amberlyst-15 and Amberlyst-36) for solid acid catalysts. The results suggest that the rates depend strongly on the acid strength of the catalysts,^{36, 38} consistent with our prior findings in HAA reaction of 2-PF with aldehydes³⁶ and conjugate addition (CA)-HAA of 2-PF with enals³⁸ without any thiol. Among all catalysts, Aquivion PW79S shows the best activity, selectivity to product **1a** and separation, and is chosen for subsequent investigation.



Scheme 2. Proposed reaction pathway for condensation of 2-pentylfuran and 2-undecanone.

Table 1. Condensation of 2-pentylfuran (2-PF) and 2-undecanone over various acid catalysts.

Entry	Catalyst	Thiol	Conv. / %		Yield / %						Formation rate of 1a / mol _{1a} mol _{H⁺} ⁻¹ h ⁻¹
			2-PF	2-Undecanone	1a	1b	1c	1d	1e	1f	
1	Auqivion PW79S	-	99	57	49	1.8	8.0	0.7	1.1	2.3	11.7
2	Auqivion PW98	-	92	51	45	1.6	8.8	0.6	0.9	3.0	5.8
3	Auqivion PW79S	1-Propanethiol	99	78	72	1.3	4.9	0.2	0.1	0.4	16.8
4	Auqivion PW98	1-Propanethiol	97	78	71	1.5	4.1	0.1	0.2	0.6	11.9
5	Amberlyst-15	1-Propanethiol	37	25	21	0.3	3.2	0.0	0.0	0.3	2.4
6	Amberlyst-36	1-Propanethiol	25	13	9.3	0.3	3.2	0.0	0.0	0.2	0.7
7	H ₂ SO ₄	1-Propanethiol	10	9.9	5.9	0.0	0.5	0.0	0.0	0.0	0.5
8	CH ₃ SO ₃ H	1-Propanethiol	21	21	14	0.0	0.5	0.0	0.0	0.0	1.2
9	<i>p</i> -TSA	1-Propanethiol	84	75	64	4.2	2.1	0.2	0.0	0.2	7.0
10	CF ₃ SO ₃ H	1-Propanethiol	>99	84	51	20	0.2	0.0	0.2	0.3	117.9

Reaction conditions: 4 mmol 2-PF, 2 mmol undecanone, 0.063 mmol H⁺ ([H⁺] was kept fixed by adjusting the amount of catalysts, *e.g.*, 0.05 g Aquivion PW79S), SH/H⁺=1 (molar ratio), 65 °C, 4 h. The rates are calculated at low conversion of 2-PF (<32%).

3.2 Effect of 1-propanethiol on product distribution

Next, we conduct time-dependent experiments with and without 1-propanethiol to elucidate the effect of the thiol (Figure 1). In the presence of 1-propanethiol, the 2-PF and 2-undecanone conversions are higher as is the yield to the dominant product, **1a**. The hydroxyalkylation product was not observed. A small fraction of **1b** forms *via* furan ring-opening of **1a** at longer times, probably due to the acid catalyzed hydrolysis in the presence of water, a byproduct of the condensation reaction. Water also promotes the self-condensation of 2-PF to produce **1c**, **1d**, **1e**, and **1f**. **1c** is the main side-product. Noticeably, the self-condensation of 2-PF, likely in the form of humins, is also higher without 1-propanethiol, a fact corroborated with the darker color of the solution (Figure S1) and the recovered catalyst after 4 h reaction. These results indicate that the thiol remarkably suppresses the self-condensation of 2-PF and further formation of humins. An overall reaction network is proposed in Scheme 2.

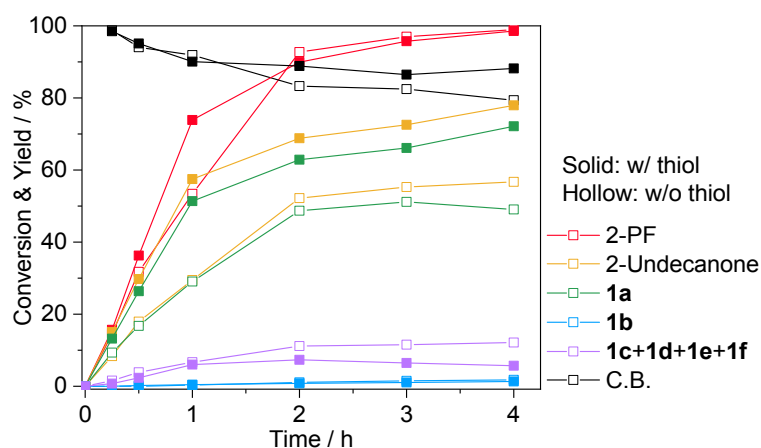


Figure 1. Time course of condensation of 2-pentylfuran (2-PF) and 2-undecanone over Aquivion PW79S. Reaction conditions: 4 mmol 2-PF, 2 mmol 2-undecanone, 0.05 g Aquivion PW79S (0.063 mmol H⁺), SH/H⁺=1 (molar ratio), 65 °C. C.B. = carbon balance.

3.3 Reaction mechanism and effect of thiol

To further understand the effect of thiol, we performed vacuum electronic structure calculations and compared the energetics of the reaction between 2-MF and the protonated acetone with and without thiol in the system. We have made the reasonable assumption that protonation of the acetone molecule is fast and thereby kinetically inconsequential. The reaction mechanisms are drawn in Scheme 3. All free energies are reported at 65 °C. Images of all intermediates and transition states are provided in the SI (Figures S2, S3).

In the absence of thiol (Scheme 3(a)), the nucleophilic addition of 2-MF to the carbonyl group (transition state TS1) is practically non-activated. The slow step of the condensation reaction between 2-MF and acetone is the dehydration of intermediate **B** (transition state TS2), which entails proton transfer from the furan ring C5 to the carbonyl oxygen of the ketone and requires *ca.* 32 kcal/mol of *intrinsic* activation free energy. The corresponding free energy profile is shown in Figure 2(a) (black line), from which we see an *apparent* activation free energy of *ca.* 22 kcal/mol with respect to the reference state of separated reactants. Although the reaction was run in a solventless environment and the experimental studies did not show signs of autocatalysis (*viz.*, no induction period was observed), we nevertheless investigated whether water produced in the course of the reaction could facilitate the proton transfer in

transition state TS2. The water molecule does not affect the nucleophilic attack on the protonated acetone (TS1) but does accelerate the dehydration of the intermediate **B** by *ca.* 22 kcal/mol, bringing the intrinsic free energy barrier down to *ca.* 10 kcal/mol (Figure 2(a), red line).

We investigated two possible ways in which addition of thiol could accelerate the kinetics of the 2-MF-acetone condensation reaction and suppress the self-condensation of 2-MF. One would be the thiol acting as a proton transfer mediating agent, similar to water. The second is thiolation of the acetone prior to the nucleophilic addition, in addition to the thiol facilitating the requisite proton transfers. As a proton transfer mediating agent, thiol is almost as effective as water (see Figure 2(a), green line), as the dehydration of the intermediate **B** to **C** requires a mere 12 kcal/mol of activation.

If thiolation of the acetone is considered as an alternative mechanism (Scheme 3(b)), we see reduction in the reaction barriers (Figure 2(b), black line), even without proton shuttling mediated by water or thiol. Although the thiolation of acetone and formation of **E** introduces a relatively high barrier (*ca.* 23 kcal/mol), due to the required water removal (TS3), it seems that it is kinetically more facile to de-thiolate **F** to **C** than dehydrate **B** to **C**, by a substantial 8 kcal/mol (*cf.* Figure 2(b), black line, TS5, and Figure 2(a), black line, TS2); the relatively high 32 kcal/mol barrier is reduced to the moderate barrier of 24 kcal/mol. Thus, thiolation of the acetone prior to the nucleophilic attack is overall beneficial. If in addition we consider thiol as a proton transfer mediator, then both the thiolation of the acetone (**D** to **E**) and the de-thiolation of the product of the nucleophilic addition (**F** to **C**) are significantly accelerated. Specifically, TS3 is reduced by 16 kcal/mol, from 23 to 7 kcal/mol, and TS5 is reduced by 11 kcal/mol, from 24 to 13 kcal/mol (compare the black and green energy profiles in Figure 2(b)). Even though the experiments in the presence of thiol did not suggest autocatalytic phenomena, we nevertheless investigated water as a proton transfer facilitating agent. Compared to proton transfer mediation by the thiol, water reduces the TS3 and TS5 barriers by an additional *ca.* 2-3 kcal/mol (Figure 2(b), red line).

To summarize, thiolation of the acetone prior to the nucleophilic attack by the furan is surely beneficial—more so when the thiol molecule mediates the requisite proton transfers as well. Although water produced from the reaction can facilitate proton transfer—in fact, it does so slightly more effectively than thiol—our experiments do not suggest an induction period and thereby rather preclude this pathway. According to Nikbin *et al.*³⁹, the self-condensation of 2-MF to **1c** (Scheme 2) requires *ca.* 20 kcal/mol of activation energy, which is significantly higher than the kinetic barriers for 2-MF-acetone condensation in the presence of thiol.

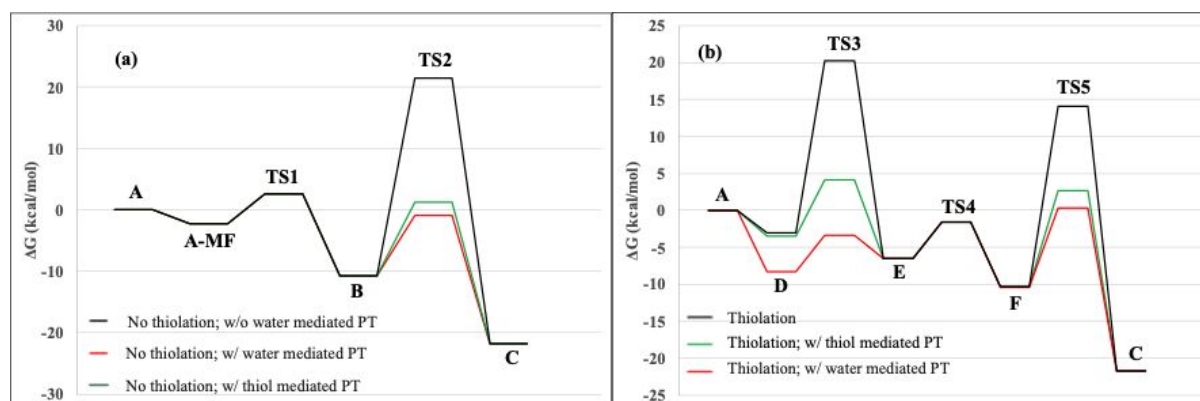
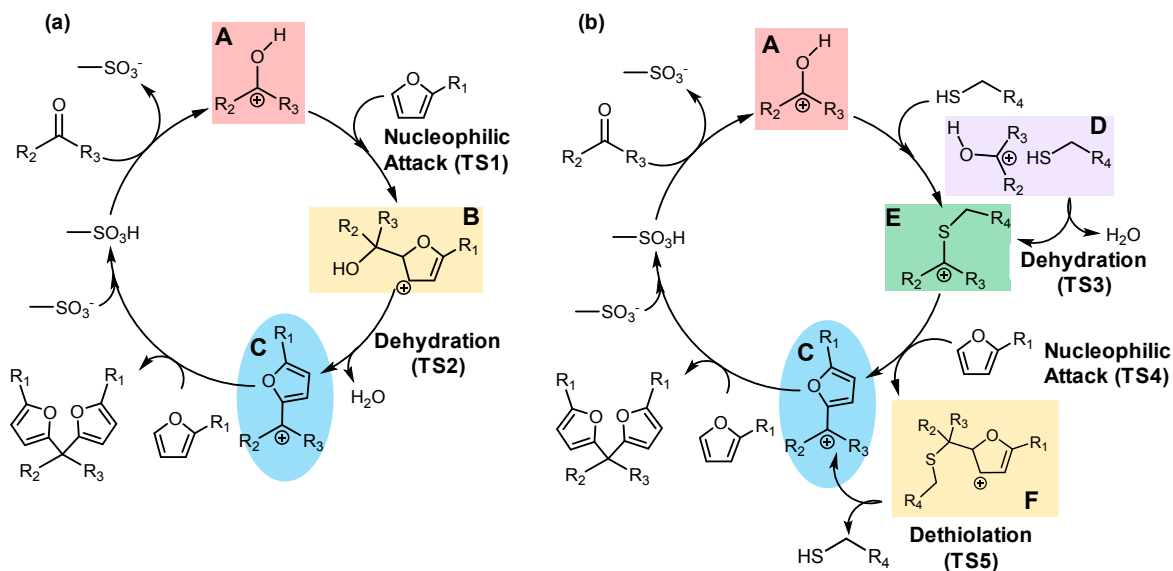


Figure 2. Free energy profiles for condensation of 2-methylfuran with protonated acetone. (a) Condensation following the Scheme 3(a) mechanism, without proton shuttling (black line) and with proton shuttling mediated by water (red line) or thiol (green line). (b) Condensation between 2-methylfuran and thiolated acetone (Scheme 3(b) mechanism) without proton shuttling (black line) and with proton shuttling mediated by water (red line) or thiol (green line). (Free energies are reported at 65 °C and are referenced to separated reactants.)



Scheme 3. Proposed reaction mechanism for the condensation of 2-alkylfuran with ketone without (a) and with (b) thiol.

3.4 Effect of thiol promoters with different substituents

To further validate the mechanism of the catalytic reaction, thiol promoters with different substituents were used for the condensation of 2-PF and 2-undecanone over Aquivion PW79S (Figure 3). At high conversions of 2-PF, all the linear thiols (1-propanethiol, 1-butanethiol, 1-hexanethiol and 1-octanethiol), cyclohexanethiol and phenylmethanethiol demonstrate better yield of product **1a** and conversion of 2-undecanone, especially 1-propanethiol, than those without thiol. *tert*-Butyl mercaptan does not promote the reaction. The formation rate of **1a** is linearly correlated to the Taft-type steric (Figure 3b) and the carbon number of linear thiols (Figure 3c) but poorly correlated with the electronic parameter $-\sigma^*$ ^{40, 41} (Figure S4). The rate decreases in the order: 1-propanethiol > 1-butanethiol > phenylmethanethiol > 1-hexanethiol > cyclohexanethiol \approx 1-octanethiol > *tert*-butyl mercaptan. This suggested the reaction rate is mainly influenced by steric effects, which agrees with previous studies on the catalytic condensation of phenol with actone/levulinic acid^{42, 43}. This is also consistent with our mechanism and that the intermediate **E** (Scheme 3b) with the higher steric hindrance slows down the reaction rate.

To further prove the promotion by thiol, diethyl sulfide was used for the reaction. The catalytic performance and the formation rate of **1a** with diethyl sulfide are similar to those without thiol, suggesting no promotion effect. This result indicates that the formation of intermediate **E** (Scheme 3b) is likely a prerequisite for the 2-alkylfuran nucleophilic attack and controls the overall reaction.

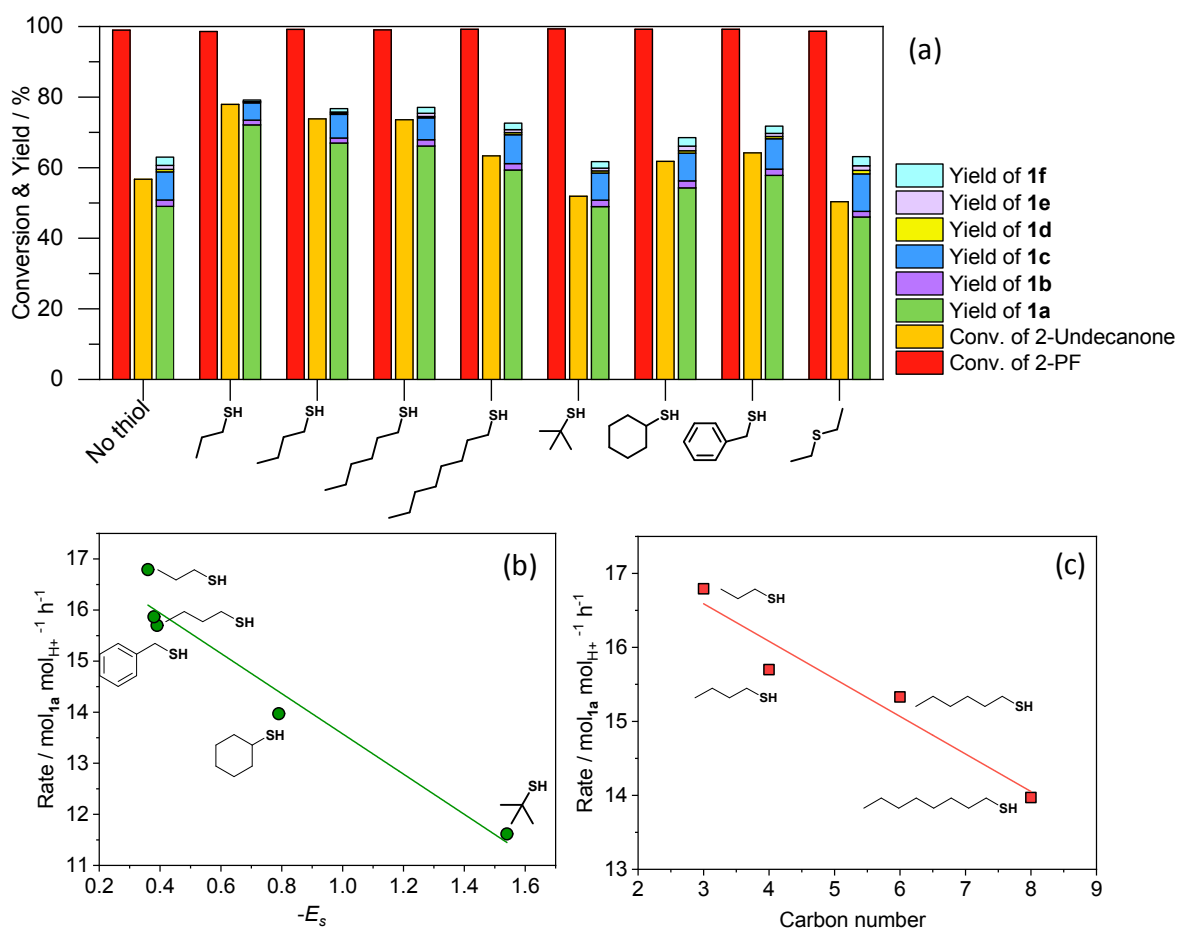


Figure 3. (a) Effect of thiol promoters with different substituents on the condensation of 2-pentylfuran (2-PF) and 2-undecanone. Reaction conditions: 4 mmol 2-PF, 2 mmol undecanone, 0.05 g Aquivion PW79S (0.063 mmol H⁺), SH/H⁺=1 (molar ratio), 65 °C, 4 h. Formation rates of **1a** vs. the Taft steric parameter $-E_s$ (b) and the carbon number of linear chain thiols (c) over Aquivion PW79S. The rates are calculated at low conversion of 2-PF (<32%).

3.5 Effect thiol to proton ratio

To further assess the mechanism, we investigated the effect of the thiol to proton ratio (Figure 4). The formation rate of **1a** increases with increasing the thiol to proton thiol/H⁺ molar ratio (Figure 4a) and is 2.2 times higher at molar ratio of 2 compared to that without thiol. The results indicate that the reaction favors the thiol cycle (Scheme 3b) as the concentration of thiol increases. These findings are also consistent with the overall reaction being controlled by formation of a sulfur-stabilized intermediate (**E** in Scheme 3), and not by proton transfer steps. Likewise, at high conversion of 2-PF, the conversion of 2-undecanone and the yield of **1a** increase first with increasing thiol to proton molar ratio (Figure 4b) and then level off at a molar ratio of around 1.

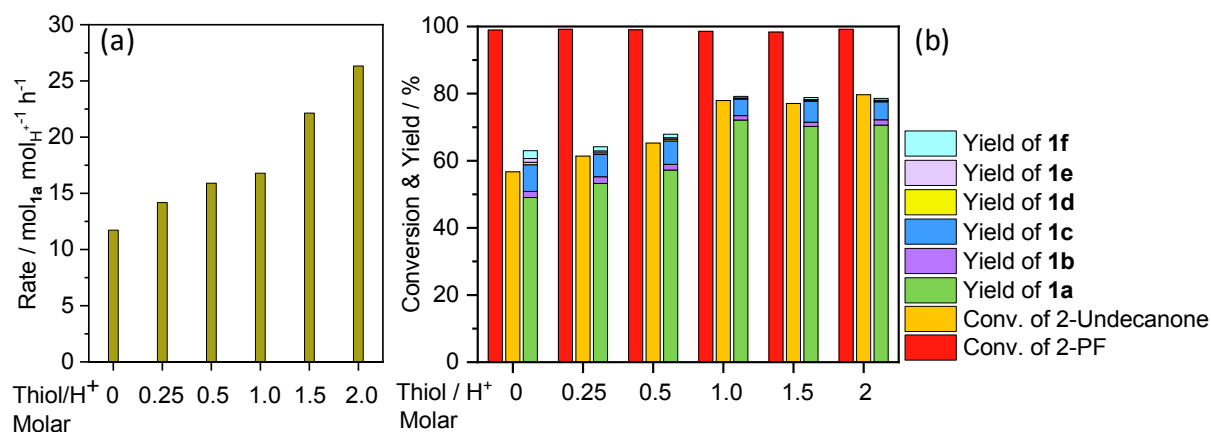


Figure 4. Effect of molar ratio of thiol to proton: (a) formation rate of **1a** and (b) performance at high conversion 2-pentylfuran (2-PF) with addition of 1-propanethiol. Reaction conditions: 4 mmol 2-PF, 2 mmol 2-undecanone, 0.05 g Aquivion PW79S (0.063 mmol H⁺), 65 °C, 4 h. The rates are calculated at low conversion of 2-PF (<32%).

3.6 Reusability of Aquivion PW79S Catalyst

Recyclability assessment of Aquivion PW79S was conducted. The catalyst was allowed to settle down and the liquid product was pipetted out after each cycle. The recovered catalyst was washed thoroughly with cyclohexane to remove surface-adsorbed unreacted reactants, 1-propanethiol and products, dried in a vacuum oven at 60 °C for 1 h, and then reused in the next cycle. Before each cycle, fresh 1-propanethiol was added to keep the same molar ratio of thiol and proton (1:1). Under comparable conditions, the catalyst achieves a similar conversion of 2-PF in five consecutive cycles, but the yield of product **1a** decreased slightly (7% loss) in the 5th cycle. ATR-IR and TGA characterizations for both the fresh and used catalysts were performed. ATR-IR spectra (Figure S5) show the characteristic bands of Aquivion PW79S. The S-O stretching at about 1000 cm⁻¹ and the C-C and C-F stretching at 1100-1300 cm⁻¹ were conserved over the catalytic runs⁴⁴. Additional bands at 2800-3000 cm⁻¹ (C-H stretching), 1580-1680 cm⁻¹ (C=C stretching), and 1380-1480 cm⁻¹ (C-H bending) were observed on the used catalysts, and their intensity increased with the number of catalytic runs. These bands could arise from polymeric 2-PF (humins) adsorption. Formation of humins is supported also by the difference in TGA decomposition profiles (mass loss) of the used catalyst after the 5th cycle and the fresh catalyst (Figure S6). The small deactivation of the catalyst after the 5th cycle is likely due to the coverage of the active sites by adsorbed humins.

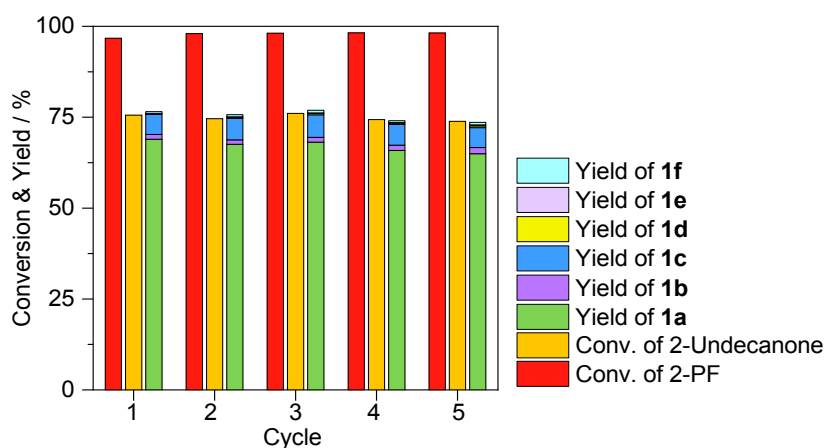
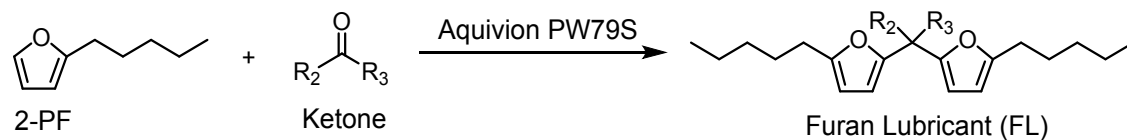


Figure 5. (a) Reusability of Aquivion PW79S in the condensation of 2-pentylfuran and 2-undecanone over Aquivion PW79S in the presence of 1-propanethiol. Reaction conditions: 4 mmol 2-pentylfuran, 2 mmol 2-undecanone, 0.05 g Aquivion PW79S (0.063 mmol H⁺), SH/H⁺=1 (molar ratio), 65 °C, 4 h.

3.7 Effect of substrates

Because commercial base oils contain a mixture of C₂₀-C₅₀ hydrocarbons, we synthesized C₂₄-C₂₉ furan-containing base oils from 2-PF and ketones of different molecular sizes and structures. The HAA reaction of 2-PF with 2-undecanone, 4-undecanone, and 6-undecanone produced C₂₉-FLs with different structures (C₂₉-FL1, C₂₉-FL2, C₂₉-FL3; see Table 2, entries 1-3). The conversion of 2-PF after 4 h of reaction is similar. However, 4-undecanone and 6-undecanone give much lower rates and yields to C₂₉-FL2 and C₂₉-FL3 than those using 2-undecanone, suggesting that steric hindrance of the alkyl chain strongly affects the reaction. Next, we investigate the HAA reaction of methyl-ketones of different carbon number, *e.g.*, 2-undecanone, 2-nonanone, and 2-hexanone, to obtain C₂₄-C₂₉ FLs. The yields of the corresponding FLs and their formation rates followed the order 2-undecanone < 2-nonanone < 2-hexanone (Table 2, entries 1, 4 and 5), correlating to their steric hindrance. The yield of C₂₄-FL could reach up to 90% in the presence of 1-propanethiol using 2-hexanone as the ketone. When a cyclic ketone (4-propylcyclohexanone) was used as a reagent, the formation rate of C₂₇-FL2 was remarkably higher than that with 2-nonanone (Table 2, entries 4 and 6), which could be due to lower steric hindrance of reagent due to the rigid cyclic ring. Steric hindrance of the ketones likely affects the stability of the intermediate (intermediate B, Scheme 3) preceding the rate-limiting dehydration step, and therefore alters the reactivity through destabilization of the dehydration transition state. The addition of 1-propanethiol enhanced the formation rates of FLs in all cases by ca. 1.2-2 times. The reaction rate is accelerated by 1.2 times with 1-propanethiol addition for 4-propylcyclohexanone (Table 2, entry 6) and almost 2 times using 4-undecanone and 6-undecanone (Table 2, entries 2 and 3). The yield of C₂₇-FL2 at high conversion of 2-PF is independent of 1-propanethiol (Table 2, entry 6). In contrast, the yields of C₂₉-FLs are double when 1-propanthiol is added for 4-undecanone and 6-undecanone (Table 2, entries 2 and 3). Together, the data shows that the kinetic promotion effect (on reaction rates) of thiol is more pronounced when steric hindrance is larger.

Table 2. HAA of 2-pentylfuran with various ketones over Aquivion PW79S with or without 1-propanethiol.

Entry	Ketone	Product	With 1-propanethiol			Without 1-propanethiol				
			Conv. / %		Yield of product / %	Formation rate / mol mol _{H⁺} h ⁻¹	Conv. / %		Yield of product / %	Formation rate / mol mol _{H⁺} h ⁻¹
			2-PF	Ketone			2-PF	Ketone		
1		C ₂₉ -FL1	99	78	72	16.8	99	57	49	11.7
2		C ₂₉ -FL2	98	36	33	4.5	98	11	11	2.5
3		C ₂₉ -FL3	99	34	33	5.5	99	9.1	8.6	2.6
4		C ₂₇ -FL1	99	88	83	22.3	>99	67	67	13.1
5		C ₂₄ -FL	>99	94	90	32.7	>99	83	82	16.1
6		C ₂₇ -FL2	98	>99	90	106.6	>99	99	97	87.6

Reaction conditions: 4 mmol 2-PF, 2 mmol ketone, 0.05 g Aquivion PW79S (0.063 mmol H⁺), SH/H⁺=1 (molar ratio), 65 °C, 4h. The rates are calculated at low conversion of 2-PF (<32%).

3.8 Properties of synthesized lubricant base oils

The key properties of C₂₉-FL1, C₂₄-FL, C₂₇-FL1 and C₂₇-FL2, as obtained from the HAA reaction of 2-PF with 2-hexanone, 2-nonanone, 2-undecanone, and 4-propylcyclohexanone respectively, were determined following various ASTM methods described in the experimental section. Table 3 compares their properties against those of commercial alkylnaphthalene base oils (ExxonMobil AN5 and KING Industries KR-007A) and a furan containing bio-ester base oil, isooctyl furan dicarboxylate (Isooctyl-FD), produced *via* esterification of FDCA and 2-ethylhexanol over *p*-TSA. For FLs with linear alkyl chain (C₂₄-FL, C₂₇-FL1 and C₂₉-FL1), the viscosities and VI increase while the Noack volatility decreases with an increase in the carbon number of base oils. This can be explained by the larger London dispersion forces increasing with increasing molecular weight^{6,45}. The PP and the oxidative stability of these FLs are similar. The C₂₇-FL2 with a cyclic ring in the structure has a higher viscosity and a lower PP and Noack volatility compared to those of C₂₇-FL1 with a linear alkyl chain⁴⁵. The oxidative stability of C₂₇-FL2 with a cyclic ring is lower than that of C₂₇-FL1 with a linear alkyl chain, which can be ascribed to the unsaturated properties of the cyclic ring.

C₂₉-FL1 has similar viscosities as the commercial synthetic alkylnaphthalene base oils (ExxonMobil AN5 and KING KR-007A) and the bio-ester base oil (Isooctyl-FD), but a higher VI. The VI, a unitless measure of the change of viscosity with temperature, is used to characterize the viscosity-temperature behavior of lubricant base oils. The higher the VI, the less the viscosity is affected by changes in temperature. Thus, our synthetic base oil has better viscosity performance than the commercial products on these metrics. The Noack Volatility of the C₂₉-FL1 is slightly higher than that of the ExxonMobil AN5 product. However, the PP of C₂₉-FL1 is much lower than that of all commercial base oils, indicating their promising performance for low temperature applications.

Table 3. Properties of synthesized base oils, commercial synthetic alkylnaphthalene base oils, and a furan-containing bio-ester base oil.

Lubricant	KV ₁₀₀ ^a (cSt)	KV ₄₀ ^a (cSt)	VI ^b	PP ^c (°C)	Noack Volatility ^d / wt%	DSC oxidation onset T ^e / °C
C ₂₄ -FL	2.85	13.30	31	<-60	49.0	145.5
C ₂₇ -FL1	3.16	14.19	74	<-60	27.7	147.4
C ₂₇ -FL2	4.15	24.18	46	-45	22.1	126.2
C ₂₉ -FL1	3.95	19.21	99	<-60	16.9	142.6
ExxonMobil AN5 ^f	4.7	29.0	74	-39	12.7	-
KING KR- 007A ^g	3.8	22.0	26	-48	-	-
Isooctyl-FD ^h	4.48	31.32	4.5	-13	-	-

^aKV100 and KV40 are kinematic viscosities at 100 °C and 40 °C, respectively (ASTM D445). ^bVI: Viscosity index calculated from KV100 and KV40 (ASTM D2270). ^cPP: Pour point (ASTM D97). ^dVolatility (ASTM D6375). ^eOxidation stability (ASTM E2009, method B, 500 psi O₂). ^fCommercial alkylnaphthalene base oil AN5

manufactured by ExxonMobil. ^aCommercial alkylnaphthalene base oil KR-007A manufactured by King Industrials, Inc. ^bA furan containing bio-ester base oil, isooctyl furan dicarboxylate (Isooctyl-FD), produced via esterification of FDCA and 2-ethylhexanol. Properties of commercial products and Isooctyl-FD were obtained from products' specifications datasheet disclosed by the manufacturers and literature³⁵, respectively.

4. Conclusions

We introduced a novel catalytic C-C coupling route via hydroxyalkylation/alkylation (HAA) to produce renewable furan-containing lubricant base oils with excellent yields (up to 90%) from biomass-derived 2-alkylfurans and ketones. Unlike aldehydes used in HAA that we reported before, ketones are less reactive. However, the use of thiols as promoters can significantly improve performance. Among several catalysts screened, Aquivion PW79S combined with 1-propanethiol as the promoter, shows the best enhancement of reaction rates, yield to the desired base oil, and catalyst stability. The reaction rates correlate well with the catalysts' acidic strength. Thiols or ketones with less steric effects substantially enhance the reaction rate and the yield to base oils. Electronic structure calculations indicate that the promotion effect of thiol results from reducing the barrier of the rate-limiting dehydration step. The synthesized base oils have similar or superior properties to the commercial synthetic alkylnaphthalene base oils and furan-containing bio-ester lubricant base oils. Importantly, the properties can be tuned by tailoring the molecular structure of base oils using different ketones. The high selectivity of the desired route provides an opportunity to make not only renewable molecules but with specific branching to tailor their properties. This work contributes to producing bio-based lubricant base oils for high performance applications.

Conflicts of interest

The authors have reported part of this work in an international patent application (WO 2019/036663 A1).

Acknowledgments

This work was supported as part of the Catalysis Center for Energy Innovation, an Energy Frontier Research Center funded by the U. S. Department of Energy, Office of Science, Office of Basic Energy Sciences under Award Number DE-SC0001004. The authors acknowledge the Advanced Materials Characterization Laboratory at the University of Delaware.

References

1. M. A. Hossain, M. A. Mohamed Iqbal, N. M. Julkapli, P. San Kong, J. J. Ching and H. V. Lee, *RSC. Adv.*, 2018, **8**, 5559-5577.
2. C. J. Reeves, A. Siddaiah and P. L. Menezes, *Journal of Bio- and Tribo-Corrosion*, 2017, **3**, 11.
3. J. E. Rorrer, A. T. Bell and F. D. Toste, *ChemSusChem*, 2019, **12**, 2835-2858.
4. S. Shylesh, A. A. Gokhale, C. R. Ho and A. T. Bell, *Acc. Chem. Res.*, 2017, **50**, 2589-2597.
5. N. A. Zainal, N. W. M. Zulkifli, M. Gulzar and H. H. Masjuki, *Renew. Sustain. Energy Rev.*, 2018, **82**, 80-102.

6. L. R. Rudnick, *Synthetics, Mineral Oils, and Bio-Based Lubricants: Chemistry and Technology, Second Edition*, 2013, CRC Press, Taylor&Francis.
7. A. Kujawska, J. Kujawski, M. Bryjak and W. Kujawski, *Renewable and Sustainable Energy Reviews*, 2015, **48**, 648-661.
8. S. M. Lee, J. Oh, B.-S. Hurh, G.-H. Jeong, Y.-K. Shin and Y.-S. Kim, *Journal of Food Science*, 2016, **81**, C2915-C2922.
9. D. Risner, E. Tomasino, P. Hughes and L. Meunier-Goddik, *Journal of Dairy Science*, 2019, **102**, 202-210.
10. P. Anbarasan, Z. C. Baer, S. Sreekumar, E. Gross, J. B. Binder, H. W. Blanch, D. S. Clark and F. D. Toste, *Nature*, 2012, **491**, 235.
11. S. Sreekumar, Z. C. Baer, A. Pazhamalai, G. Gunbas, A. Grippo, H. W. Blanch, D. S. Clark and F. D. Toste, *Nature Protocols*, 2015, **10**, 528.
12. F. Huang, Z. Liu and Z. Yu, *Angewandte Chemie International Edition*, 2016, **55**, 862-875.
13. L. Rakers, F. Schäfers and F. Glorius, *Chemistry – A European Journal*, 2018, **24**, 15529-15532.
14. A. Corma, M. Renz and C. Schaverien, *ChemSusChem*, 2008, **1**, 739-741.
15. C. A. Gaertner, J. C. Serrano-Ruiz, D. J. Braden and J. A. Dumesic, *Journal of Catalysis*, 2009, **266**, 71-78.
16. T. N. Pham, T. Sooknoi, S. P. Crossley and D. E. Resasco, *ACS Catalysis*, 2013, **3**, 2456-2473.
17. T. Arai, M. Tamura, Y. Nakagawa and K. Tomishige, *ChemSusChem*, 2016, **9**, 1680-1688.
18. S. Liu, Y. Okuyama, M. Tamura, Y. Nakagawa, A. Imai and K. Tomishige, *Green Chem.*, 2016, **18**, 165-175.
19. S. Liu, Y. Okuyama, M. Tamura, Y. Nakagawa, A. Imai and K. Tomishige, *ChemSusChem*, 2015, **8**, 628-635.
20. A. Corma, O. de la Torre and M. Renz, *Energy & Environmental Science*, 2012, **5**, 6328-6344.
21. Y. L. Louie, J. Tang, A. M. L. Hell and A. T. Bell, *Applied Catalysis B: Environmental*, 2017, **202**, 557-568.
22. J. Dijkmans, W. Schutyser, M. Dusselier and B. F. Sels, *Chemical Communications*, 2016, **52**, 6712-6715.
23. W. Schutyser, S. Van den Bosch, J. Dijkmans, S. Turner, M. Meledina, G. Van Tendeloo, D. P. Debecker and B. F. Sels, *ChemSusChem*, 2015, **8**, 1805-1818.
24. X. Chang, C. Zhang, L. Gao, X. Liu, S. You, W. Qi, K. Wang, X. Guo, R. Su, H. Lu and Z. He, *Transactions of Tianjin University*, 2019, **25**, 488-496.
25. S. Sadula, A. Athaley, W. Zheng, M. Ierapetritou and B. Saha, *ChemSusChem*, 2017, **10**, 2566-2572.
26. Y. M. Questell-Santiago, R. Zambrano-Varela, M. Talebi Amiri and J. S. Luterbacher, *Nature Chemistry*, 2018, **10**, 1222-1228.
27. M. Kim, Y. Su, A. Fukuoka, E. J. M. Hensen and K. Nakajima, *Angewandte Chemie International Edition*, 2018, **57**, 8235-8239.
28. K. A. Goulas, A. V. Mironenko, G. R. Jenness, T. Mazal and D. G. Vlachos, *Nature Catalysis*, 2019, **2**, 269-276.

29. R. Mariscal, P. Maireles-Torres, M. Ojeda, I. Sádaba and M. López Granados, *Energy & Environmental Science*, 2016, **9**, 1144-1189.
30. D. S. Park, K. E. Joseph, M. Koehle, C. Krumm, L. Ren, J. N. Damen, M. H. Shete, H. S. Lee, X. Zuo, B. Lee, W. Fan, D. G. Vlachos, R. F. Lobo, M. Tsapatsis and P. J. Dauenhauer, *ACS Cent. Sci.*, 2016, **2**, 820-824.
31. M. Balakrishnan, G. E. Arab, O. B. Kunbargi, A. A. Gokhale, A. M. Grippo, F. D. Toste and A. T. Bell, *Green Chem.*, 2016, **18**, 3577-3581.
32. S. Shylesh, A. A. Gokhale, K. Sun, Adam M. Grippo, D. Jadhav, A. Yeh, C. R. Ho and A. T. Bell, *Sustain. Energy Fuels*, 2017, **1**, 1805-1809.
33. M. Balakrishnan, E. R. Sacia, S. Sreekumar, G. Gunbas, A. A. Gokhale, C. D. Scown, F. D. Toste and A. T. Bell, *Proceedings of the National Academy of Sciences*, 2015, **112**, 7645-7649.
34. M. Gu, Q. Xia, X. Liu, Y. Guo and Y. Wang, *ChemSusChem*, 2017, **10**, 4102-4108.
35. M. Fan, J. Ai, S. Zhang, C. Yang, X. Du, P. Wen, X. Ye, F. Zhou and W. Liu, *Friction*, 2019.
36. S. Liu, T. R. Josephson, A. Athaley, Q. P. Chen, A. Norton, M. Ierapetritou, J. I. Siepmann, B. Saha and D. G. Vlachos, *Sci. Adv.*, 2019, **5**, eaav5487.
37. M. J. T. Frisch, G. W.; Schlegel, H. B.; Scuseria, G. E.; Robb, M. A.; Cheeseman, J. R.; Scalmani, G.; Barone, V.; Mennucci, B.; Petersson, G. A.; Nakatsuji, H.; Caricato, M.; Li, X.; Hratchian, H. P.; Izmaylov, A. F.; Bloino, J.; Zheng, G.; Sonnenberg, J. L.; Hada, M.; Ehara, M.; Toyota, K.; Fukuda, R.; Hasegawa, J.; Ishida, M.; Nakajima, T.; Honda, Y.; Kitao, O.; Nakai, H.; Vreven, T.; Montgomery, J., J. A.; Peralta, J. E.; Ogliaro, F.; Bearpark, M.; Heyd, J. J.; Brothers, E.; Kudin, K. N.; Staroverov, V. N.; Keith, T.; Kobayashi, R.; Normand, J.; Raghavachari, K.; Rendell, A.; Burant, J. C.; Iyengar, S. S.; Tomasi, J.; Cossi, M.; Rega, N.; Millam, J. M.; Klene, M.; Knox, J. E.; Cross, J. B.; Bakken, V.; Adamo, C.; Jaramillo, J.; Gomperts, R.; Stratmann, R. E.; Yazyev, O.; Austin, A. J.; Cammi, R.; Pomelli, C.; Ochterski, J. W.; Martin, R. L.; Morokuma, K.; Zakrzewski, V. G.; Voth, G. A.; Salvador, P.; Dannenberg, J. J.; Dapprich, S.; Daniels, A. D.; Farkas, O.; Foresman, J. B.; Ortiz, J. V.; Cioslowski, J.; Fox, D. J., *Gaussian 09, Revision D.01*, 2013, Gaussian, Inc., Wallingford CT.
38. S. Liu, B. Saha and D. G. Vlachos, *Green Chemistry*, 2019, **21**, 3606-3614.
39. N. Nikbin, S. Caratzoulas and D. G. Vlachos, *Appl. Catal. A: Gen.*, 2014, **485**, 118-122.
40. R. W. Taft, *Journal of the American Chemical Society*, 1952, **74**, 3120-3128.
41. R. W. Taft, *Journal of the American Chemical Society*, 1953, **75**, 4538-4539.
42. R. K. Zeidan, V. Dufaud and M. E. Davis, *Journal of Catalysis*, 2006, **239**, 299-306.
43. S. Van de Vyver, S. Helsen, J. Geboers, F. Yu, J. Thomas, M. Smet, W. Dehaen, Y. Román-Leshkov, I. Hermans and B. F. Sels, *ACS Catalysis*, 2012, **2**, 2700-2704.
44. A. Karam, K. De Oliveira Vigier, S. Marinkovic, B. Estrine, C. Oldani and F. Jérôme, *ACS Catal.*, 2017, **7**, 2990-2997.
45. J. Israelachvili, *Intermolecular and Surface Forces 3rd Edition*, 2011, Academic Press, Elsevier Inc.

TOC Graph

Furan-containing lubricants with excellent yields (up to 90%) were synthesized by hydroxylalkylation/alkylation (HAA) of biomass derived 2-alkylfurans with ketones over a solid acid and a thiol promoter.

